Precision Engineering 37 (2013) 443–450

Contents lists available at SciVerse ScienceDirect

Precision Engineering

journal homepage: www.elsevier.com/locate/precision

Surface finishing of intricate metal mould structures by large-area electron beam irradiation

J.W. Murray[a], P.K. Kinnell[a], A.H. Cannon[b], B. Bailey[b], A.T. Clare[a,*]

[a] Precision Manufacturing Centre, Department of M3, University of Nottingham, Nottingham, NG7 2RD, United Kingdom
[b] Hoowaki LLC, 511 Westinghouse Road, Pendleton, SC 29670, USA

ARTICLE INFO

Article history:
Received 3 July 2012
Received in revised form 19 October 2012
Accepted 25 November 2012
Available online 19 December 2012

Keywords:
Electron beam melting
Electron beam irradiation
Surface textured mould tools
Precision polishing

ABSTRACT

The advancement of polymer moulding tools is increasingly focused on imparting not only form but also surface texture for functionality to the surfaces of parts that are created. Furthermore, the increasing demand for inexpensive and higher quality micro-components means that tools for replication processes must take advantage of advanced manufacturing techniques. Tools created by processes such as micro-investment casting, as in this case, may often suffer from excessive surface roughness, malformed edges and general deformation. This results in higher de-moulding forces and a reduction in fidelity of moulded parts to design intent. In this study, large-area electron beam irradiation (EB) is shown to be an effective technique for improving these metrics. For the first time, large population, high aspect ratio micro-features are subject to this process and the mechanisms of smoothing and key enhancement phenomena are demonstrated. The possibility of including EB irradiation in an integrated process chain for arriving at net shape is also discussed.

Surfaces of protruding features are shown to have surface roughness reduced significantly from 126 to 22 nm Ra value, with bottom substrate also similarly improving from 150 to 27 nm Ra. Bottoms of recessed features are also observed to have much improved surface finishes. 'Doming' of tops of column features is also demonstrated, further enhancing form. These features would be far too fragile to be polished by any other mechanical method.

1. Introduction

The ability of replication/moulding techniques, to create micro-components and micro featured components is continually improving. This is largely driven by consumer demands for plastic components with enhanced performance or functionality [1]. Surface microstructures can affect the properties of a surface, including tribological characteristics such as coefficient of friction and wear [2], appearance and optical characteristics [3], heat transfer coefficient during boiling and condensation [4], and water repellency [5–9]. Micromoulding is a scalable route to manufacturing microstructured surfaces [10–12]. The requirements for scaling micromoulding tools to high volume applications are that the moulding tools must be made of durable metal such as steel and be of low cost.

Increasing pressure is being placed on suppliers to produce so called 'micro' components or indeed larger components which include microstructures. For such components or features on components to be produced in large volumes and within the customer price expectation replication technologies are the only viable methodology. Recent moulding technologies have been increasingly focused upon designing intricate microstructures in metal moulds [13–15] in order to impart enhanced surface properties upon the final polymer part such as increased hydrophobicity [14,16] Metal microstructures and nanostructures are attractive for micro-manufacturing moulds [17] as they can be reused many times more than moulds composed of traditional microfabrication materials such as silicon or quartz. Embossing, moulding, rolling, and stamping can produce microstructures at 1/1000 the cost of conventional fabrication techniques such as silicon microfabrication, micro-milling, or laser micromachining. Unlike paint, spray, or plasma-based surface finishes, micromoulding can fabricate lithographically defined and ordered three dimensional microstructures [10–12].

With increasing demands for higher form accuracy and lower surface roughness of produced parts, technologies for the finishing of mould tools have been the subject of much research [18]. A rapid and predictable ejection mechanism during mechanical separation at the end of the moulding process is also vital to the repeatability of the operation and the quality of the finished part and it is known that higher surface roughness increases friction coefficients and the

* Corresponding author at: Room A49, Coates Building, University Park, University of Nottingham, NG7 2RD, United Kingdom. Tel.: +44 115 951 4109.
E-mail address: adam.clare@nottingham.ac.uk (A.T. Clare).

0141-6359/$ – see front matter. Crown Copyright © 2012 Published by Elsevier Inc. All rights reserved.
http://dx.doi.org/10.1016/j.precisioneng.2012.11.007

required de-moulding forces between tool and moulded part [19]. The surface finishing of intricate, precision components is therefore highly important.

For flat surfaces, ultrasonic polishing, an adaptation of ultrasonic machining has been demonstrated using an abrasive slurry and a CNC tool [20,21], with an Ry roughness of 7 nm achievable, although the size of the tool and abrasive nature of the process limits this from being applied to intricate, non-flat surfaces. Laser polishing has also been applied to the finishing of both flat milled tool steel [22] and structured moulds [18] since it is a non-mechanical polishing process, although a roughness of approximately 0,5 μm was achieved, much higher than that from abrasive techniques on flat surfaces. Laser polishing also requires a focused beam and its rastering across the surface, and a significant remelted and heat-affected zone is produced. Electro-chemical polishing (ECP) [23] has also been demonstrated as a potential technique for the process, although it is not desirable since it is time consuming, asperity dependent and incurs an environmental burden. Effluent resulting from ECP presents a significant disposal challenge.

Large-area electron beam irradiation has been demonstrated as a highly efficient method of polishing metal mould surfaces, and is capable of finishing surfaces machined by laser beam [24] and EDM [25,26] with improved corrosion behaviour observed. Since it is a pulsed process and the heating/cooling cycle usually occurs in under 10 μs, repetition of the irradiation process is used to gradually achieve the finish, and a large remelted/recrystallised zone is not produced. Because of this, the process is suited to the polishing of intricate structures for which their intended form must be retained. The process is also clean with no material wastage, requires no precise set-up procedure and takes place in a vacuum, eliminating the possibility of oxidation. In this work we apply for the first time the electron irradiation technique to the polishing of highly intricate and high-aspect ratio metal mould structures. This paper reports an investigation into the application of electron beam parameters to the change in form and surface roughness of metal mould structures. X-ray diffraction (XRD) is also used to interrogate the surface microstructure and expose any phase or crystallographic texture changes induced by the process.

Table 1
Specimens subjected to electron beam irradiation.

Sample designation	Material	Description	Dimensions (μm)
a	17-4PHA	Rods, circular	Ø80
b	17-4PHA	Holes, circular	Ø80
c	17-4PHA	Holes, circular	Ø40
d	17-4PHA	Holes, circular	Ø20
e	17-4PHA	Rods, square	25 × 25
f	17-4PHA	Rods, circular	Ø100

2. Experimental

2.1. Metal mould structures

In this study six micro-structured specimens were investigated to understand the effect of electron beam irradiation upon varying morphology. These structures have been specifically designed to introduce texture and surface functionality into plastic moulded components. A breakdown of the microstructures with dimensions can be seen in Table 1, and SEM images of each surface are presented in Fig. 1. The material used for all tests was AISI 630, [17-4PHA]. It is a precipitation hardening martensitic stainless steel with composition: Cr 15–17.5%, Ni 3–5%, Cu 3–5%, Mn, P, S, Si, Ta, Nb < 1%, C 0,07%, and Fe balance.

Typical features produced via the investment casting method were selected. This process chain begins with a rapid prototyped polymer part onto which a silicon rubber is cast. A ceramic is then cast to the microstructured rubber, after which metal is cast to the structured ceramic, resulting in a microstructured mould used to impart features on to a final polymer part.

2.2. Electron irradiation experiments

A Sodick PF32A EBM machine was used for electron beam irradiation experiments (schematic in Fig. 2). The irradiation process is carried out in an air-tight chamber into which an inert gas, Argon at a pressure of 0,05 Pa is supplied, after an initial 10 min vacuum cycle time. This Argon gas is used as the medium for plasma build up required for the electron generation and beam propagation. The

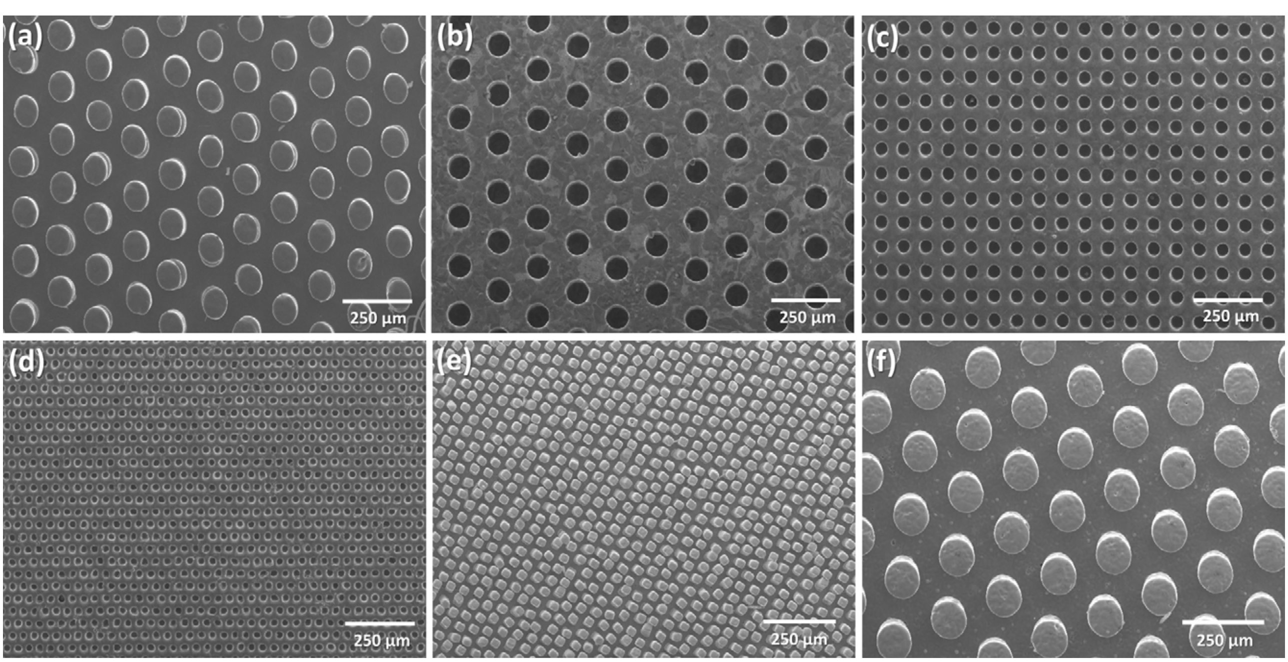

Fig. 1. Array of mould structures used in this study. Figure label corresponds to designation in Table 1.

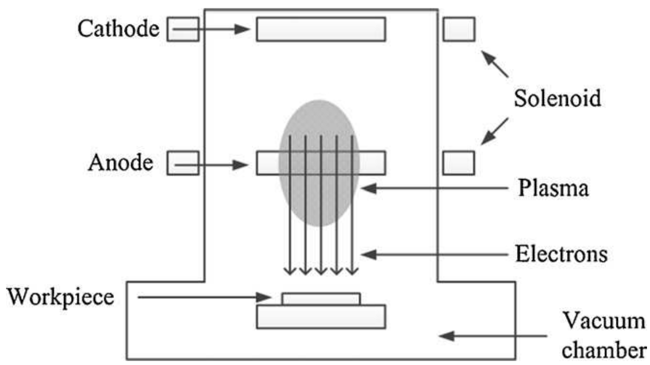

Fig. 2. Schematic of 'EBM' irradiation process.

diameter of the beam is 60 mm; with a pulse-time of 2–3 μs, pulse interval of 11 s and energy density < 10 J/cm^2. The beam has been shown to extend further than its 60 mm diameter although the energy density is significantly diminished beyond this point. Within the 60 mm diameter, energy density has shown to be uniform [25].

Firstly a solenoid coil produces a magnetic field, at the maximum intensity of which a pulsed voltage is applied to the anode. Electrons are generated by Penning ionisation and move towards the anode. Argon atoms are then ionised by repeated collisions with electrons, generating plasma near the anode. At the maximum intensity of this plasma a pulsed voltage is applied to the cathode and electrons from the plasma are accelerated by the high electric field [27]. The bombardment of electrons with the workpiece surface causes it to heat and rapidly quench.

The electron beam irradiation technique is usually employed to enhance the surface finish of large specimens as opposed to fine, high aspect ratio features, i.e. large volume components such that the electron interaction volume can be ignored. For the purposes of this experiment the volume of electron interaction (and hence molten volume) is significant with respect to feature sizes. From previous trials a recast layer of 2–10 μm can be expected with limited ablation of substrate material. This is inherent to the requirements of the EB process since it is a finishing technique and only near net shape components will be applicable to this process.

2.3. Surface characterisation

The measurement of surface roughness was conducted with a Bruker AXS 'NP Flex' white light interferometric (WLI) profilometer, and a 50× objective was used. To ensure the Ra value was not influenced by the surface form of the pillars, or any waviness present post processing was carried out on the data using the proprietary instrument analysis software. Tilt was removed from the data, and then a high pass Fourier filter using Gaussian smoothing was applied, the spatial cut off used for the filter was set to 10 μm. This had the effect of removing the waviness and form due to the domed top of the pillars, without influencing the micro roughness which was of interest. For consistency this post-processing step was applied to all data in the same way.

X-ray diffraction was performed using a Bruker AXS "D8 Advance" diffractometer, producing CuK (α) monochromatic radiation. The diffractometer was rotated through 40 to 100° with a step value of 0,025°. Microscopy was performed with a Hitachi S-2600 scanning electron microscope in secondary electron mode.

3. Results and discussion

3.1. Initial trials and graduated parameters

Initial trials were undertaken to establish a suitable process window in which to perform bulk experiments on all samples. These trials were undertaken using processing conditions detailed in Table 2. This sequence of conditions was performed on Sample *e* (square rods). This initial sequence of parameters was investigated based upon previous experimentation on several materials including CoCrMo, Ti6Al4V and SS316. The lowest cathode voltage observed to produce any detectable change in roughness in this case was between 10 and 15 kV, usually requiring multiple shots.

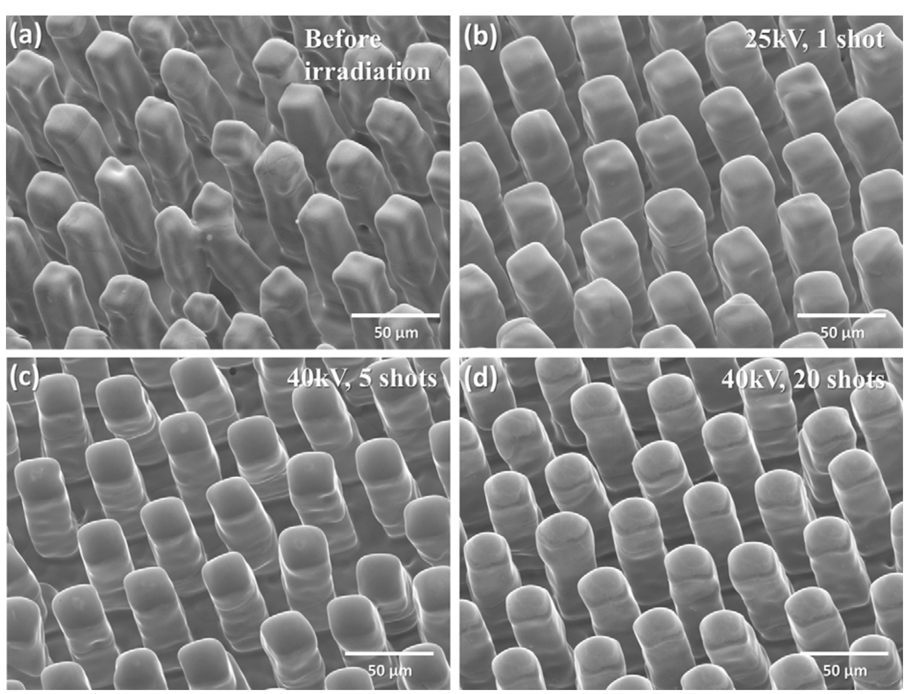

Fig. 3. Specimen *e* subjected to graduated irradiation: (a) unaffected sample, (b) subject to 1 shot at 25 kV, (c) subject to 5 shots at 40 kV, (d) subject to 20 shots at 40 kV. High uniformity, smoothing and doming is exhibited in (d).

Table 2
Initial trial – sequence of graduated parameters.

Cathode voltage (kV)	Number of shots
10, 15, 20, 25, 30, 35	1
40	1, 5, 20

Based on this the investigation of graduated parameters started with 10 kV and 1 pulse.

The sample initial condition is characterised by a variation in top surface roughness with edges appearing sharp and top surfaces which are undulating. At low shot numbers and moderate cathode voltages there is little effect on both the form and surface roughness of the rods. However, as cathode voltage and shot number increase the form and surface roughness are observed to improve. Some key observed changes in morphology and finish can be seen in Fig. 3. In this study, the structures subject to 10 and 15 kV and 1 shot showed no clear changes in morphology, only after 1 shot at 25 kV was smoothing of asperities and slight rounding of the flat tops of rods observed. After 5 shots at 40 kV, a highly smoothed finish was produced, and after a further 20 shots, a significant doming effect was observed, although with diminishing returns to a further improved finish.

To obtain a single optimum parameter to produce the best form and surface finish on all samples, the graduated parameter results were considered and a second sample (sample *f*) was subjected to 5 shots, resulting in much improved finish and with some domed morphology. It was then subjected to 25 shots, which produced once again a slightly enhanced domed form compared to 5 shots, but with little further improvement to surface finish. Based on experimentation on these samples, optimum parameters of 40 kV cathode voltage and 30 shots were determined for further testing of samples. The detailed 'EBM' parameters can be seen in Fig. 4 (Table 3).

3.2. Morphology and surface finish

Before irradiation all column tips displayed a degree of variation in both form and surface finish. An amount of the population also exhibited slanted surfaces and asperities (as seen in Figs. 3(a) and 5(a)). After irradiation with 30 shots at 40 kV cathode voltage, a much improved surface finish and high uniformity was produced on all column samples. Slanting exhibited by column tips before irradiation was much reduced and a domed shape was produced on all columns. It is thought that the domed, smooth form of the column tips will assist with reduced friction involved in the mechanical separation of mould tool and polymer part, and therefore less damage to the final part. Although improved final part fidelity to the original intended form would be expected from such mould structures subject to electron irradiation, it should be noted that this is achieved via loss of form accuracy of the shape. It should be considered that for surface treatment of features that approach the same scale as the recast depth (2–10 μm), the form of these features may be significantly affected. It is proposed that in a comprehensive manufacturing chain where process effects can be modelled, novel surface textures could be developed in this way. These may include advanced morphologies and highly localised metallurgical properties. It is thought that with further careful parameter selection, much finer features could be successfully polished.

The smoothing effect was also observed to a small extent on the side walls of columns, although the distinction between the remelted, smooth top surface is clearly defined in the lines at the bottom of the top 'cap'. This suggests that the flow of molten material after irradiation is small and even after 30 repetitions remelted material has not moved significantly to the sides of the columns. On sample *e* however (columns), a secondary region of remelted material can be seen on the sides of the columns (Fig. 4(a)), this gives insight that the beam is capable of affecting features even at a highly acute angle.

Uno et al. [28] investigated the relationship between workpiece surface tilting angle and the achievable surface roughness for a flat surface after large-area electron beam irradiation. It was found that with at a 60° angle, surface roughness achieved was almost the same as with the sample perpendicular to the beam, and even at 90°, surface roughness was halved to from 6,5 μm to approximately 3,5 μm Rz. The ability of this finishing process to improve surface roughness of metal moulds in a short period of 11 s interval between shots without re-angling the sample makes it a highly realistic option for surfaces with highly complex features.

Surfaces with recessed features before irradiation exhibited uneven ridge contours and asperities on the top surface. As can be seen in Fig. 6, after irradiation a highly smooth surface is produced on the top surface, with a gradual flow of the surface into the recesses, as opposed to sharper edges between top and sides walls of the holes. The bottoms of the recesses also exhibited improved surface finish, and asperities were removed even on sample *d* with the finest recessed features (Fig. 6(c) and (d)). The ability of a post-process to improve surface finish of such small features without damaging their form is highly unique and without requiring a precise set-up operation is entirely unique, and as feature size is reduced, the significance of surface imperfections becomes greater, and so here it is demonstrated that this finishing technique is particularly suited to the most intricate of structures.

In most materials for which electron beam irradiation has been applied, cratering is usually observed. This is the case in Cr4Mo4V steel [29], 316L austenitic stainless steel [30], NiTi alloy [31] and Al–Si alloy [32]. It has been proposed that the mechanism of formation of these craters is a combination of disparity in melting temperatures between phases and also density effect which cause 'bubbles' of lighter material to move rapidly towards the surface while the uppermost layer is molten. When this bubble breaches the surface a crater effect can be observed [32,33]. This has also been markedly observed in 316L Stainless steel by Zhang et al. [30] in their work which examines enhanced pitting corrosion resistance as a result of electron beam irradiation. In this work the craters produced by preferential melting of MnS inclusions, and the resulting craters were sensitive to corrosion, particularly if a pore remained at the centre at the point of eruption, although this effect can be lessened after further irradiation.

In the case of this study, no craters were observed on any samples, and affected surfaces were universally homogenous. This has positive implications on the corrosion behaviour of treated surfaces of this particularly stainless steel, and it is proposed the uniformity of melting points between inclusions and phases in martensitic AISI 630 steel prevented crater formation and promoted a smooth finish. In Fig. 7 surface morphology of both the bottom and top surfaces before and after irradiation can be clearly seen. No craters can be observed, and both the bottom and top surfaces have a similarly improved finish. A somewhat improved finish on the sides of the columns can also be seen.

3.3. Surface roughness

SEM observation of the samples processed using electron beam irradiation clearly demonstrated the improvement in surface finish that is achieved. To quantify the expected reduction in surface roughness which is made possible by applying the technique, a non-contact optical surface profiling technique was selected as a means of directly measuring surface roughness, Ra. This is a challenging measurement as the samples are highly profiled and display many high aspect ratio micro-scale features therefore precluding

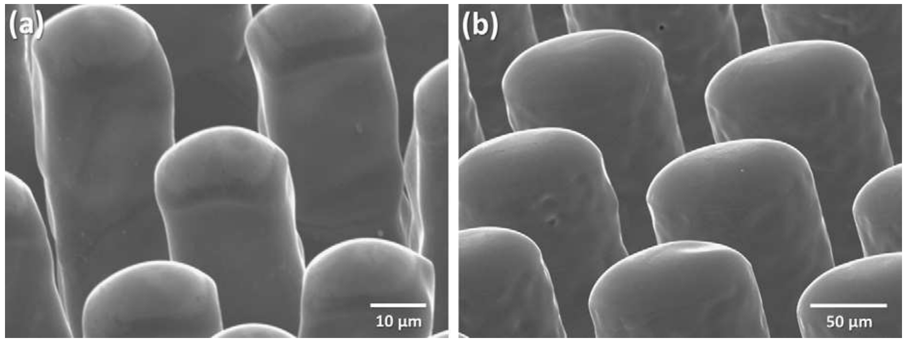

Fig. 4. 'Doming' in initial trials conducted on (a) Sample E subjected to graduated parameters and (b) Sample F subjected to 5 + 25 shots at a cathode voltage of 40 kV.

Table 3
Final experimental parameters.

Cathode voltage (kV)	Number of shots	Anode voltage (kV)	Solenoid voltage (kV)	Argon pressure (Pa)
40	30	5	1,5	0,05

the use of a stylus-based measurement technique. Thus an optical non-contact system was selected. Sample type *a* was considered for this analysis as it allowed measurements of surface roughness to be obtained from both the top and bottom of the high aspect ratio rods. As the sample constitutes an array of circular rods that are approximately 80 μm diameter, roughness measurements were performed on sample areas situated on the top surface of the pillars (approximately centrally located), as well as at the base of pillars. Sample areas were analysed from four randomly selected sites at the top of pillars, and four randomly selected sites at the base of pillars.

Surface roughness results are shown in Table 4. Final surface roughness achieved on tops of rods was between 16 nm and 29 nm Ra with a mean of 22 nm, an approximate five-fold improvement. Bottom surface improvement had a mean improvement of almost

Table 4
Surface roughness measured from samples before and after irradiation.

	Surface roughness, Ra (nm)			
	Rod top surface		Substrate	
	Before	After	Before	After
1	128.8	23.58	101.4	28.58
2	146.7	16.31	170.1	26.30
3	136.6	28.66	146.1	25.11
4	90.92	19.96	181.7	26.92
Mean	125.7	22.12	149.8	26.72

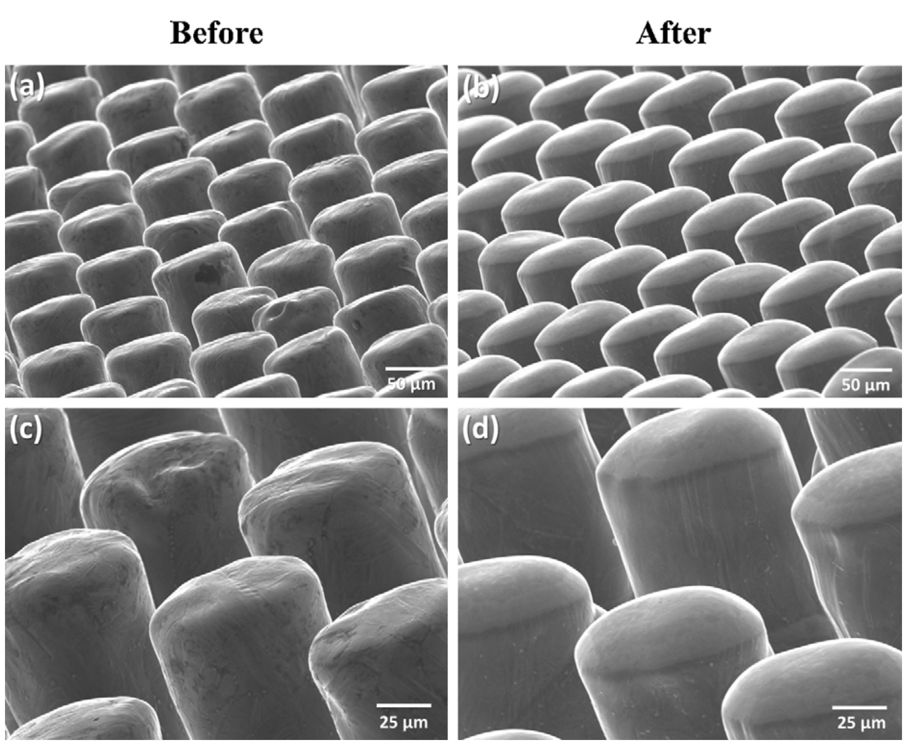

Fig. 5. Column tips on Sample *a* pre (a) and (c) and post irradiation (b) and (d). Greater uniformity is exhibited as well as enhanced doming.

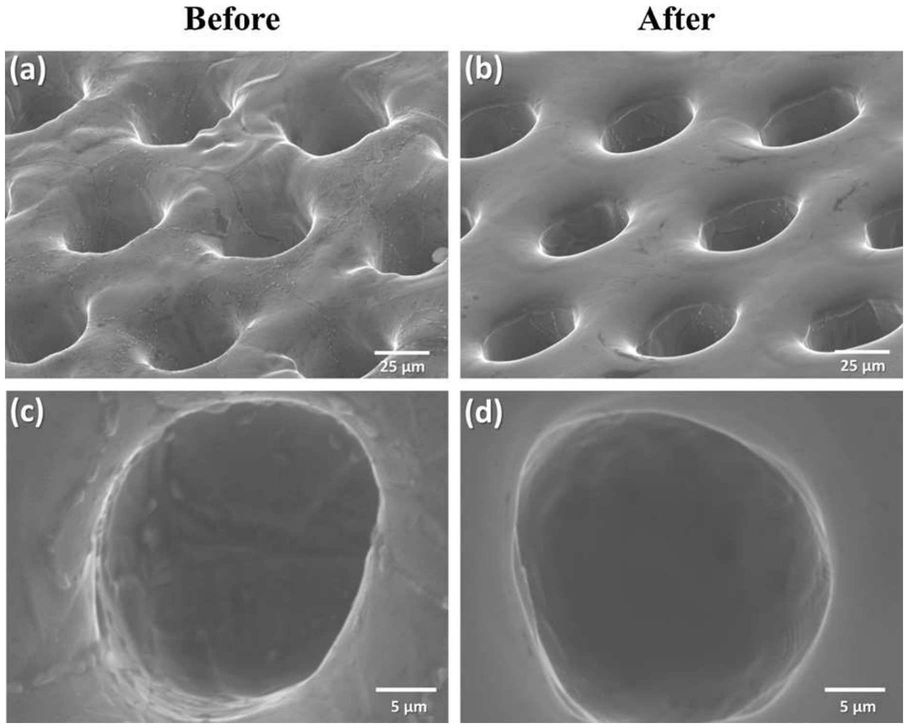

Fig. 6. Recessed features on Sample *c* (a) before and (b) after irradiation, and Sample *d* (c) before and (d) after irradiation. A significant improvement in surface roughness can be seen and asperities are eliminated on the top surface. The surface finish of the bottom of the smallest features can also be improved.

six-fold, and with smaller variation. All measurements showed a final Ra value of below 30 nm. Typical line scan profiles from the top of a rod, before and after irradiation are presented in Fig. 8.

This surface finish is comparable to that achievable by magnetorheological abrasive flow finishing (MRAFF), a process recently developed for nano-finishing. The process combines a rheological medium, a rotating magnetic field, and reciprocating motion to polish complex and internal geometries. Das et al. [34] achieved a surface roughness of 16 nm Ra on stainless steel by this method. Magnetorheological finishing has also been used to reach a final roughness of 8 nm Ra on silicon for X-ray mirror applications [35]. The ability of large-area electron beam irradiation as shown in this study to reach surface roughness values below 20 nm suggests it is a competing technology for nano-scale finishing, and may replace

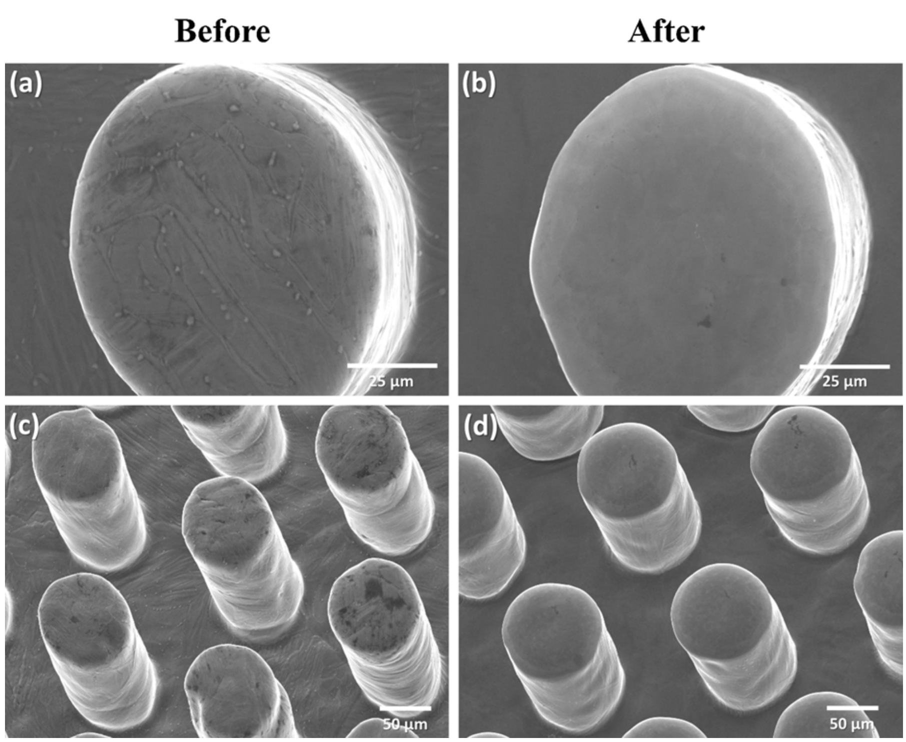

Fig. 7. Both top surfaces of rods (Sample *b*) and substrate surface can clearly be observed to have been polished. No cratering is observed.

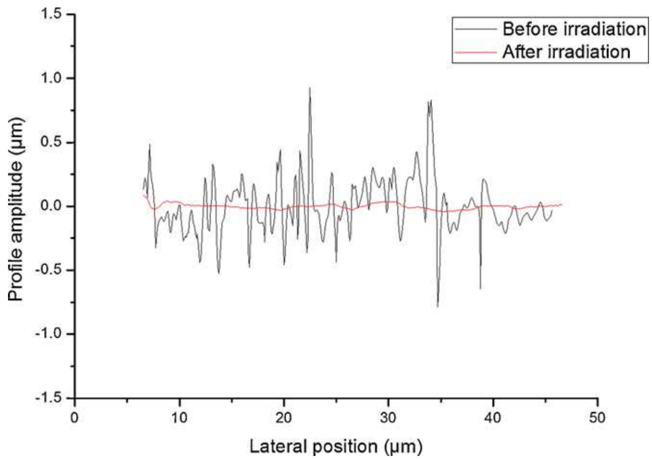

Fig. 8. Line surface profile scans showing the reduced surface roughness of column tops post EBM.

the need for more complicated and time consuming abrasive flow finishing technologies commonly used for geometries of the type discussed in this study.

Typical 3D surface profiles from the top and bottom surface of Sample *a* before and after irradiation are presented in Fig. 9. Asperities seen on both the bottom substrate and the tops of columns are eliminated after irradiation, and surface finish is clearly much improved. Surface features not observable under SEM imaging are also revealed after profiling. Tops and bottoms of the sample exhibit slightly different surface features. Some evidence of flow can be seen in Fig. 9(d), reflecting the movement of molten material towards the edge of the rods. At the bottom of the sample (Fig. 9(b)), between rods, bands can be seen. This may be explained by the flow of material from higher regions, i.e. the sides of the rods and into the substrate beneath, resulting in a concentration of material in these lower regions, and a region of compressed material remains. This effect may explain the better surface finishes achievable at the tops of rods (see Table 4), since material flow is unrestricted. Despite a duration of 2–3 μs per pulse and a high theoretical cooling rate of 10^8–10^9 K/s [36], it is clear that gravitational effects play a significant role in the smoothing and doming effect observed in this study, and with sufficient numbers of pulses, significant material displacement can occur.

3.4. XRD analysis

Since the remelted region of irradiated surfaces is typically between 2–10 μm, and significant microstructural refinement is expected to occur, TEM analysis is usually required for detailed microstructural analysis of the surface layer. However, XRD analysis is a useful technique to determine any phase changes and preferential crystal orientation introduced by the process. XRD was therefore performed on a flat sample of the mould material before and after irradiation by 30 shots at 40 kV cathode voltage, the same parameters as used on the microstructured moulds. The results of this are shown in Fig. 10.

XRD results were normalised so that the (2 0 0) peaks for both samples were equal in order to more clearly demonstrate changes in crystalline texture. The material is a martensitic stainless steel which also contains delta ferrite. After irradiation it was found no FCC austenitic phases were formed. Since body-centred cubic delta ferrite and body-centred tetragonal martensite produce very similar XRD patterns, transformations to other BCC/BCT phases are difficult to detect by XRD [37]. Despite this, significant crystalline texture was introduced at the surface after 30 shots at highest irradiation cathode voltage of 40 kV. Of particular note is the doubling of the ratio of the intensities of the (1 1 1) to (2 0 0) peaks after irradiation, as well as the (2 2 0) to (2 0 0) ratio. Furthermore the ratio of the (2 1 1) to (2 0 0) peaks is almost tripled. The ability of the process to rapidly introduce such crystalline texture may have implications for the corrosion improvement in the material.

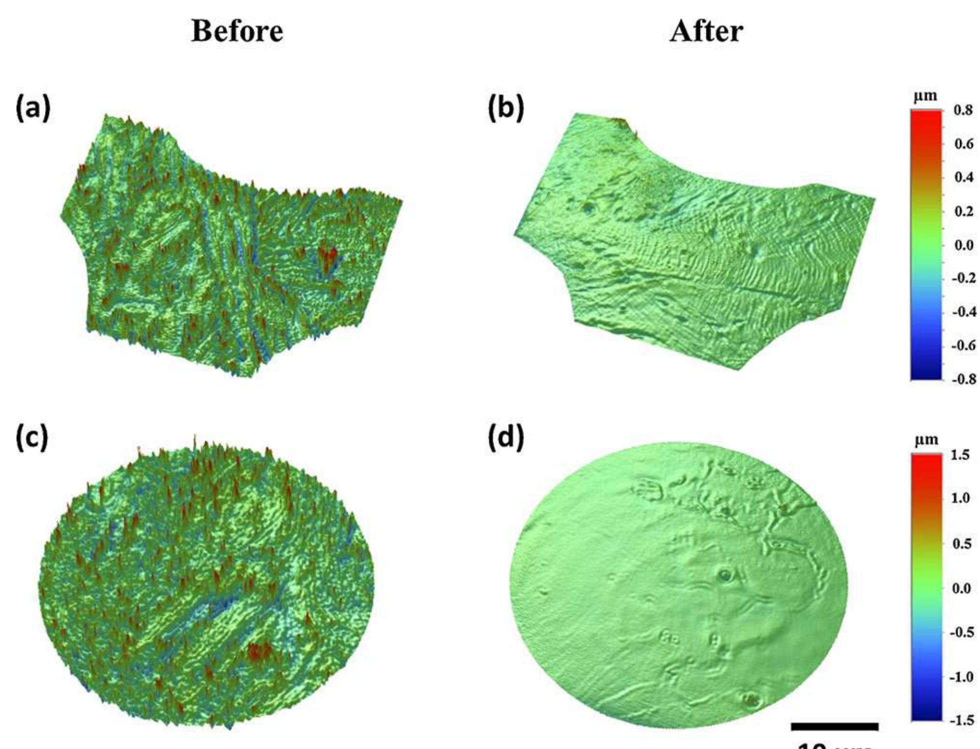

Fig. 9. 3D surface profiles of bottoms and tops of micro-rods (a) and (c) before, and (b) and (d) after irradiation.

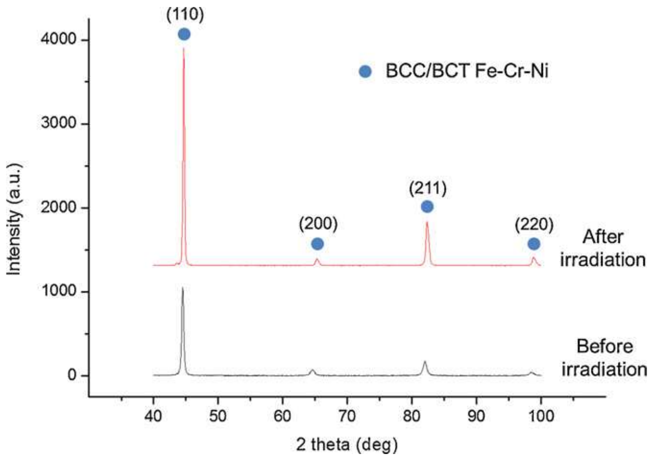

Fig. 10. X-ray analysis of irradiated and control material. No new phases are produced, however crystalline texture can be observed as a direct result of the process.

4. Conclusions

- Large-area electron beam irradiation has been shown to be an excellent method for polishing engineered surface microstructures of high aspect ratios. Since this is a noncontact method protrusions can be smoothed without damaging engineered surface microstructures and intended form of such structures can be enhanced.
- The rapidity of process, requiring 11 s per electron pulse in vacuum, makes it highly applicable for the post-processing of high-value, complex structured components.
- Top surface roughness of micro-rods is enhanced from an initial Ra 126 nm to 22 nm with no significant detrimental effect on form. Bottom surface roughness is enhanced from an initial Ra of 150 to 27 nm. This nano-scale roughness achieved suggests the process could compete with other super-finishing technologies.
- The finishing of the bottom surfaces of recesses just 20 μm diameter can be achieved.
- The morphology of finished surfaces is modified for minimal de-moulding forces. It is expected that these surfaces will also demonstrate enhanced heat transfer coefficients.
- The formation of craters is markedly not observed in micro-columns or indeed the base plane of this martensitic stainless steel. This is in contrast to other researchers' observations in a wide variety of materials in which 'cratering' is usually observed.
- X-ray diffraction results indicate that a preferred grain orientation upon resolidification can be observed in the (1 1 0) planes for the dominant phase present in this material.

References

[1] Heckele M, Schomburg WK. Review on micro molding of thermoplastic polymers. Journal of Micromechanics and Microengineering 2004;14:R1–14.
[2] Dumitru G, Romano V, Weber H, Haefke H, Gerbig Y, Pfluger E. Laser microstructuring of steel surfaces for tribological applications. Applied Physics A 2000;70:485–7.
[3] Yoshioka S, Kinoshita S. Structural or pigmentary? Origin of the distinctive white stripe on the blue wing of a Morpho butterfly. Proceedings of the Royal Society B: Biological Sciences 2006;273:129–34.
[4] Li C, Wang Z, Wang P-I, Peles Y, Koratkar N, Peterson GP. Nanostructured copper interfaces for enhanced boiling. Small 2008;4:1084–8.
[5] Cannon AH, King WP. Curvature affects superhydrophobicity on flexible microstructured polydimethylsiloxane. Denver, CO, USA: IEEE Transducers; 2009.
[6] Cannon A, Maguire M, Hulseman R, King W. Manufacturing microstructured surfaces for automotive applications. Sustainable automotive technologies 2011. Greenville, SC, USA: Springer; 2011. pp. 19–23.
[7] Cannon AH, King WP. Visualizing contact line phenomena on microstructured superhydrophobic surfaces. Journal of Vacuum Science and Technology 2010;28:L4–21.
[8] Cannon AH, King WP. Hydrophobicity of curved microstructured surfaces. Journal of Micromechanics and Microengineering 2010;20:025018.
[9] Cannon AH, Maguire M, King WP. Freeform microstructured stainless steel molds. In: ASPE 2011 spring topical meeting: structured and freeform surfaces. Charlotte, NC: American Society for Precision Engineering; 2011. p. 147–9.
[10] Cannon AH, King WP. Microstructured metal molds fabricated via investment casting. Journal of Micromechanics and Microengineering 2010;20:025025.
[11] Cannon AH, Allen AC, Graham S, King WP. Molding ceramic microstructures on flat and curved surfaces with and without embedded carbon nanotubes. Journal of Micromechanics and Microengineering 2006;16:2554–63.
[12] Cannon AH, King WP. Casting metal microstructures from a flexible and reusable mold. Journal of Micromechanics and Microengineering 2009;19:095016.
[13] Cannon AH, King WP. Microstructured metal molds fabricated via investment casting. Journal of Micromechanics and Microengineering 2010;20:7.
[14] Cannon AH, King WP. Casting metal microstructures from a flexible and reusable mold. Journal of Micromechanics and Microengineering 2009;19, 095016.
[15] Yoon Y, Lee DW, Lee JB. Surface modified nano-patterned SU-8 pillar array optically transparent super-hydrophobic thin film. Journal of Micromechanics and Microengineering\ 2012;22, 035012.
[16] Cannon AH, King WP. Hydrophobicity of curved microstructured surfaces. Journal of Micromechanics and Microengineering 2010;20, 025018.
[17] Makela T, Haatainen T, Majander P, Ahopelto J, Lambertini V. Continuous double-sided roll-to-roll imprinting of polymer film. Japanese Journal of Applied Physics 2008;47:5142–4.
[18] Brinksmeier E, Riemer O, Gessenharter A, Autschbach L. Polishing of structured molds. CIRP Annals – Manufacturing Technology 2004;53:247–50.
[19] Pouzada AS, Ferreira EC, Pontes AJ. Friction properties of moulding thermoplastics. Polymer Testing 2006;25:1017–23.
[20] Hocheng H, Kuo KL. Fundamental study of ultrasonic polishing of mold steel. International Journal of Machine Tools and Manufacture 2002;42:7–13.
[21] Suzuki H, Moriwaki T, Okino T, Ando Y. Development of ultrasonic vibration assisted polishing machine for micro aspheric die and mold. CIRP Annals – Manufacturing Technology 2006;55:385–8.
[22] Ukar E, Lamikiz A, López de Lacalle LN, del Pozo D, Arana JL. Laser polishing of tool steel with CO_2 laser and high-power diode laser. International Journal of Machine Tools and Manufacture 2010;50:115–25.
[23] Sun JJ, Taylor EJ, Srinivasan R. MREF-ECM process for hard passive materials surface finishing. Journal of Materials Processing Technology 2001;108: 356–68.
[24] Selada A, Manaia A, Vieira MT, Pouzada AS. Effect of LBM and large-area EBM finishing on micro-injection moulding surfaces. International Journal of Advanced Manufacturing Technology 2011;52:171–82.
[25] Uno Y, Okada A, Uemura K, Raharjo P, Furukawa T, Karato K. High-efficiency finishing process for metal mold by large-area electron beam irradiation. Precision Engineering 2005;29:449–55.
[26] Uno Y, Okada A, Okamoto Y. Surface modification of EDMed surface by wide-area electron beam irradiation. Journal of Japan Society of Engineering Education 2003;51:58–61.
[27] Okada A, Uno Y, Uemura K, Raharjo P, McGeough JA. Surface modification for orthopaedic titanium alloy by wide-area electron beam. Proceedings of the Institution of Mechanical Engineers Part B: Journal of Engineering Manufacture 2007;221:173–8.
[28] Uno Y, Okada A, Uemura K, Raharjo P, Sano S, Yu Z, et al. A new polishing method of metal mold with large-area electron beam irradiation. Journal of Materials Processing Technology 2007;187–188:77–80.
[29] Xu F, Guo G, Tang G, Ma X, Wang L, Ozur GE, et al. Microstructure modifications and corrosion behaviors of Cr4Mo4V steel treated by high current pulsed electron beam. Materials Chemistry and Physics 2011;126:904–8.
[30] Zhang K, Zou J, Grosdidier T, Dong C, Yang D. Improved pitting corrosion resistance of AISI 316L stainless steel treated by high current pulsed electron beam. Surface and Coatings Technology 2006;201:1393–400.
[31] Zhang KM, Zou JX, Grosdidier T, Gey N, Yang DZ, Hao SZ, et al. Surface modification of Ni (50.6% at.%) Ti by high current pulsed electron beam treatment. Journal of Alloys and Compounds 2007;434–435:682–5.
[32] Walker J, Murray J, Narania S, Clare A. Dry sliding friction and wear behaviour of an electron beam melted hypereutectic Al–Si alloy. Tribology Letters 2012;45:49–58.
[33] Qin Y, Dong C, Wang XG, Hao SZ, Wu AM, Zou JX, et al. Temperature profile and crater formation induced in high-current pulsed electron beam processing. Journal of Vacuum Science and Technology A 2003;21: 1934–8.
[34] Das M, Jain VK, Ghoshdastidar PS. Nano-finishing of stainless-steel tubes using rotational magnetorheological abrasive flow finishing process. Machining Science and Technology 2010;14:365–89.
[35] Sidpara A, Jain VK. Nano-level finishing of single crystal silicon blank using magnetorheological finishing process. Tribology International 2012;47: 159–66.
[36] Qin Y, Zou J, Dong C, Wang X, Wu A, Liu Y, et al. Temperature-stress fields and related phenomena induced by a high current pulsed electron beam. Nuclear Instruments and Methods in Physics Research Section B: Beam Interactions with Materials and Atoms 2004;225:544–54.
[37] Schroeder R, Hammes G, Binder C, Klein AN. Plasma debinding and sintering of metal injection moulded 17-4PH stainless steel. Materials Research 2011;14:564–8.